Reconstruction of flows past airfoils near stall based on scarce pressure data

Cynthia Tayeh, Vincent Mons, Olivier Marquet

RECONSTRUCTION OF FLOWS PAST AIRFOILS NEAR STALL BASED ON SCARCE PRESSURE DATA

C. Tayeh[1], *V. Mons* [1] *and O. Marquet*[1]

[1] *DAAA, ONERA, Université Paris Saclay, F-92190 Meudon, France*

cynthia.tayeh@onera.fr

Abstract

This study investigates the application of variational data assimilation to reconstruct the mean flow over a NACA4412 airfoil at a chord-based Reynolds number of $Re_c = 3.5 \cdot 10^5$. The flow configuration exhibits challenging features such as strong separation and recirculation at the trailing edge, which are not accurately captured by baseline Reynolds-Averaged Navier-Stokes (RANS) models. The key finding of this study is the potential of the data assimilation technique to accurately reconstruct the mean reference flows obtained from high-fidelity simulations (DNS) based on the observation of wall pressure. The reconstruction process is validated by first observing all the synthetic pressure data, then by using only a limited number of these wall data, and eventually relying on a single pressure observation. Remarkably, favorable performance is achieved even when using a single pressure measurement. Overall, this research emphasizes the potential of data assimilation in reconstructing complex turbulent flows based on RANS simulations and very sparse pressure data. The results demonstrate the effectiveness of this approach in enhancing the accuracy of mean flow predictions, particularly in challenging flow configurations characterized by separation and recirculation.

1 Introduction

Experimental fluid dynamics and scale-resolved calculations are commonly used approaches for studying real-world flow phenomena. However, experimental measurements are often limited in space and time and may not provide a full description of the flows of interest, while scale-resolved calculations such as Direct Numerical Simulations (DNS) can be computationally expensive. Reynolds-Averaged Navier-Stokes (RANS) methods provide a faster alternative but suffer from modeling deficiencies, particularly in predicting complex flow phenomena such as strong separation and recirculation near stall. Data assimilation (DA) techniques have emerged as a promising tool to address these limitations by combining experimental results and RANS simulations to improve flow predictions. This includes adjusting model coefficients or introducing corrective fields in the RANS equations [13], as well as using observation data from high-fidelity simulations or experiments [4, 8].

While most DA studies in the RANS framework have focused on velocity data, only few studies have examined the use of wall pressure measurements, which include [8, 11, 1, 9, 2]. Despite this increasing interest in using wall data, the quantitative assessment of reconstructed mean flows using such data is still limited, especially for complex flow configurations for the majority of studies that have relied on wall data. This study aims to investigate the potential of data assimilation to accurately estimate complex turbulent mean flows using RANS and limited wall data. The flow configuration considered in this study is the flow past a NACA4412 airfoil at a chord-based Reynolds number of $Re_c = 3.5 \cdot 10^5$ near-stall. These flow conditions exhibit significant separation and recirculation at the trailing edge, which are not adequately captured by popular RANS models. Synthetic wall measurements are obtained from the recent Direct Numerical Simulations (DNS) conducted by Gleize et al. [6]. These DNS data are also used to assess the quality of the reconstructed mean flows by data assimilation and for validation purposes.

In this paper, we first describe the flow configuration, the reference DNS results, the RANS model, and the data assimilation approach for mean-flow reconstruction in section 2. Section 3 then presents the data assimilation results, with a focus on the case where only a single pressure data is considered for reconstruction. Finally, section 4 provides concluding remarks and discusses future perspectives.

2 Flow configuration and data assimilation methodology

DNS results

Recently, Direct Numerical Simulations (DNS) were performed by Gleize et al. [6] to obtain a detailed database of trailing-edge separated flows near stall for a NACA4412 airfoil. The simulations were carried out at a chord-based Reynolds number of $Re_c = 3.5 \times 10^5$ and an almost incompressible flow regime with an infinite upstream Mach number of 0.117. The study focused on various angles of incidence denoted by α, specifically in the pre-stall regime.

Special attention was given to triggering the laminar-turbulent transition while minimizing distur-

bances to the flow. This was achieved by introducing small cylindrical roughness elements evenly distributed in the spanwise direction on the suction and pressure sides of the airfoil. By placing the roughness elements at specific locations (5% and 50% chord on the suction and pressure sides, respectively) for the considered angles of attack (8°, 10°, 11°), the development of a laminar separation bubble near the leading edge was avoided, and transition to turbulence was induced.

The mean flow fields at $\alpha = 8^\circ$ and $\alpha = 11^\circ$ obtained from the DNS results, are displayed in the top row of figure 1. It can be seen that turbulent trailing-edge separation is already present for $\alpha = 8^\circ$, and this separation becomes more pronounced as the angle of attack increases. Such mean flows form reference results and will be used for validation purpose and the goal of the following data assimilation methodology will be to reconstruct these full mean flows using the synthetic pressure measurements.

Baseline RANS results

To provide a more cost-effective alternative to DNS, one may consider the Reynolds-Averaged Navier-Stokes (RANS) models. In this context, we rely on the widely-used Spalart-Allmaras turbulence model [12], which was primarily developed for aerodynamic applications. This model uses the Boussinesq hypothesis to close the RANS equations. It introduces an equation for an eddy-viscosity-like variable, denoted as $\tilde{\nu}$, which allows to derive the actual eddy-viscosity field that affects the RANS momentum equations. RANS simulations are performed based on a finite element-based implementation in the software FreeFEM++ ([7], detailed in [5]). Additionally, two stabilization methods, namely Streamline-Upwind Petrov-Galerkin (SUPG) finite elements [3] and Grad-Div [10], are employed.

The mean flow that is obtained through the RANS simulations based on the Spalart-Allmaras turbulence model is illustrated in the bottom row of figure 1. A comparison between the RANS and DNS results reveals noticeable discrepancies near the trailing edge at $\alpha = 8^\circ$, that become significant at $\alpha = 11^\circ$ where RANS fails to accurately capture the recirculation region. This comparison highlights the limitations of the RANS approach in capturing complex flow phenomena accurately, especially in regions with recirculation. In addition, the differences in pressure coefficient (C_p) between the RANS and DNS simulations can be detected in figure 2 leading in particular to a large overestimation of lift obtained by RANS compared to DNS ($C_L = 1.40$ versus $C_L = 1.26$).

Data assimilation procedure

The limitations associated with predicting the reference flow using the RANS model have been discussed in the previous subsection. To address these discrepancies, a data assimilation technique that enables the RANS model to accurately estimate and reconstruct the reference flow, is presented here. First, we use the full DNS mean flow for comparison purposes then we explore the use of synthetic pressure data through a data assimilation approach. Following a methodology similar to that in Franceschini et al. [5], we introduce a corrective spatially-dependent field, denoted as $\tilde{g}$, in the governing equation of the eddy-viscosity-like variable $\tilde{\nu}$ in the Spalart-Allmaras model as follows:

$$\tilde{\mathbf{u}} \cdot \nabla\tilde{\nu} - \nabla \cdot (\eta(\tilde{\nu})\nabla\tilde{\nu}) - s(\tilde{\nu}, \nabla\tilde{\nu}, \nabla\tilde{\mathbf{u}}) = \tilde{g}\tilde{\nu}, \quad (1)$$

where $\tilde{\mathbf{u}}$ represents the mean-flow velocity field, $\eta(\tilde{\nu})$ is a diffusion coefficient, and $s(\tilde{\nu}, \nabla\tilde{\nu}, \nabla\tilde{\mathbf{u}})$ combines production, destruction, and cross-diffusion terms [12]. Notably, the corrective field $\tilde{g}$ is multiplied by $\tilde{\nu}$ in equation (1), allowing for natural focus on regions with significant turbulence intensity and facilitating adjustments in areas with high turbulence levels. The model correction $\tilde{g}$ is determined by minimizing the discrepancies between reference DNS data $\bar{\mathbf{m}}$ and the estimated quantity obtained from RANS, denoted as $\tilde{\mathbf{m}}(\tilde{g})$. This is achieved through a least-square variational data assimilation approach aiming to identify the field $\tilde{g}$ that minimizes the following cost function:

$$\mathcal{J}(\tilde{g}) = ||\bar{\mathbf{m}} - \tilde{\mathbf{m}}(\tilde{g})||^2_{\mathcal{M}}, \quad (2)$$

where $||\cdot||_{\mathcal{M}}$ represents the norm associated with the observation space. In this study, the reference data $\bar{\mathbf{m}}$ primarily corresponds either to a full DNS mean flow (for purpose comparisons) or to the pressure coefficient C_p. In this case, $||\cdot||_{\mathcal{M}}$ corresponds to the Euclidean norm for $\mathbb{R}$. The minimization of $\mathcal{J}$ with respect to the model correction is achieved using an iterative gradient-based descent method. The low-memory Broyden-Fletcher-Goldfarb-Shanno (L-BFGS) method is chosen for the descent algorithm. Note that the gradient of $\mathcal{J}$ with respect to $\tilde{g}$ is computed using an adjoint approach to account for the equality constraint imposed by the RANS equations.

3 Results

We now apply the mentioned data assimilation methodology to reconstruct the mean flow at $\alpha = 11^\circ$ using pressure observations extracted from DNS. The main objective of this section will be to identify and discuss an effective strategy for obtaining satisfactory flow reconstruction results based on synthetic pressure observations. For comparison purposes, we will also present the results when considering the full DNS mean-velocity field. In this case, $\bar{\mathbf{m}} = \bar{\mathbf{u}}_d$ where $\bar{\mathbf{u}}_d$ refers to the DNS mean velocity field. This initial test will allows to assess the accuracy of the corrected term $\tilde{g}$ in reconstructing the mean reference flow. It will also enables to compare the results obtained when dense velocity measurements and sparse pressure measurements are used. Next, we will proceed to a more

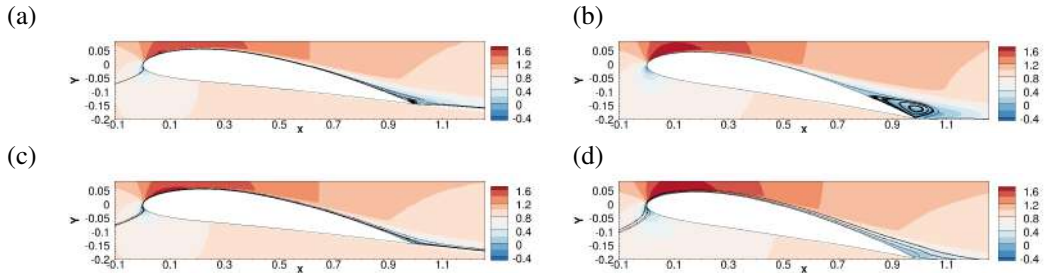

Figure 1: Streamwise mean velocity obtained with (a)-(b) DNS or (c)-(d) baseline RANS. Left and right columns correspond to $\alpha = 8^\circ$ and $\alpha = 11^\circ$, respectively. Streamlines are shown with black curves to highlight the recirculation region at the trailing edge.

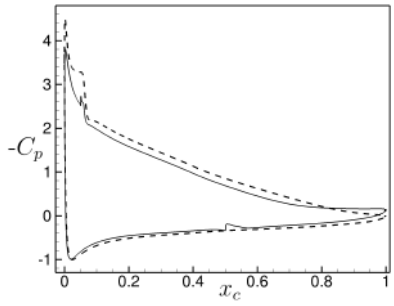

Figure 2: Pressure coefficient C_p obtained from DNS (solid line), and baseline RANS (dash line) at $\alpha = 11^\circ$.

challenging case where only wall data, such as pressure observations, will be considered. We will first investigate the use of all the DNS wall pressure observations on the suction and pressure sides as the observation $\bar{\mathbf{m}}$ in the data assimilation procedure, i.e ($\bar{\mathbf{m}} = C_p(\mathbf{x})$). We recall that the DNS pressure coefficient C_p is presented in figure 2 with black solid line. Subsequently, we will explore a more realistic case where 27 pressure data on the suction side and 13 pressure data on the pressure side, resulting in a total of 40 data points, are considered. In this case, $\bar{\mathbf{m}} = C_p(\mathbf{x}_m^i)_{i=1,\dots,N}$, where C_p denotes the pressure coefficient extracted from DNS at $N = 40$ specific positions denoted by $\mathbf{x}_m^i$. This test will be particularly relevant because it can emulate the data available from experimental measurements, which are often limited in practice. Finally, we will explore the efficacy of using a single pressure data point in the data assimilation process to determine the minimum amount of pressure data required for accurate flow reconstruction. By systematically analyzing these different cases, we aim to identify the most effective approach for reconstructing the mean flow based on synthetic pressure observations.

To quantify the accuracy of the mean-velocity field reconstruction, we define the relative error $e_r(\tilde{\mathbf{u}})$ as the ratio of the reconstruction error $e(\tilde{\mathbf{u}})$ to the baseline error $e(\tilde{\mathbf{u}}_b)$, given by:

$$e_r(\tilde{\mathbf{u}}) = \frac{e(\tilde{\mathbf{u}})}{e(\tilde{\mathbf{u}}_b)}, \quad e(\tilde{\mathbf{u}}) = \left(\frac{\int_{\Omega_m} (\bar{\mathbf{u}}_d - \tilde{\mathbf{u}})^2 \, d\Omega_m}{\int_{\Omega_m} \bar{\mathbf{u}}_d^2 \, d\Omega_m} \right)^{\frac{1}{2}}, \tag{3}$$

where $\bar{\mathbf{u}}_d$ and $\tilde{\mathbf{u}}_b$ refer to the DNS and baseline RANS mean-velocity fields, respectively, while Ω_m is a subdomain centered around the airfoil defined as $\Omega_m = \{\mathbf{x} = (x, y);\ -0.5 < x < 1.5, -0.1 < y < 0.2\}$. The error $e_r(\tilde{\mathbf{u}})$ quantifies the improvement in velocity estimation compared to baseline RANS, with $e_r(\tilde{\mathbf{u}}_b) = 1$ indicating no improvement.

Furthermore, we define the norm of the difference between the reference DNS and the reconstructed mean velocity fields denoted by $E(\tilde{\mathbf{u}}(\mathbf{x}))$ calculated at each grid point $\mathbf{x} = (x, y)$, as follows:

$$E(\tilde{\mathbf{u}}(\mathbf{x})) = ||\bar{\mathbf{u}}_d(\mathbf{x}) - \tilde{\mathbf{u}}(\mathbf{x})|| \tag{4}$$

where $||\cdot||$ represents the Euclidean norm (L_2 norm) of the error vector at each grid point. This evaluation enables us to identify regions where the reconstruction performs well and areas that require further refinement.

Reconstruction from full or limited pressure data

Figure 3 presents a comparison of results between the baseline RANS and various data assimilation cases, including the observation of the full DNS mean velocity field, full C_p, or a limited number of C_p data points extracted from DNS. The left column shows the velocity field error norms $E(\tilde{\mathbf{u}}_b(\mathbf{x}))$ and $E(\tilde{\mathbf{u}}(\mathbf{x}))$ (see equation 4), while the right column displays the streamwise mean velocity.

From the left-hand side figures, it is evident that the velocity field error norm obtained from the baseline RANS simulation, $E(\tilde{\mathbf{u}}_b(\mathbf{x}))$ (figure 3(a)), is substantial, particularly in the trailing edge region. However, this error significantly decreases when the data assimilation technique is applied in all three cases shown in figures 3(c)(e)(g), especially when considering the full DNS mean flow for comparison. Notably, despite some error that remain when assimilating pressure data in figures 3(e)(g), the error norm is significantly reduced compared to the baseline RANS sim-

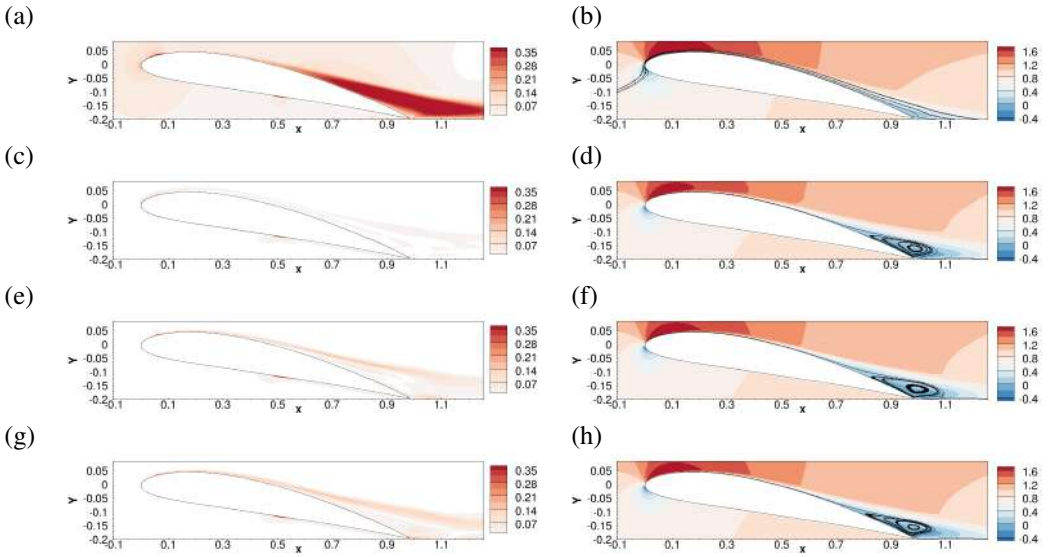

Figure 3: The norm error of the velocity field $E(\tilde{\mathbf{u}}(\mathbf{x}))$ (left columns) and the streamwise mean velocity (right columns) obtained with (a)-(b) baseline RANS, (c)-(d) RANS assimilated using the full DNS mean flow, (e)-(f) RANS assimilated using the full synthetic C_p of DNS, (g)-(h) RANS assimilated using pointwise C_p of DNS (total of 40 data). Streamlines are shown with black curves to highlight the recirculation region at the trailing edge.

ulation. Even when the number of pressure measurements is decreased to a total of 40 data points (figure 3(g)), the velocity error norm $E(\tilde{\mathbf{u}}(\mathbf{x}))$ remains approximately similar to the case where all synthetic pressure data points are considered (figure 3(e)). Now focusing on the figures in the right column, it can be observed that a significant recirculation region is clearly obtained for the three assimilation cases, even when considering only limited pressure measurements (figure 3(h)), which was not the case with the baseline RANS (figure 3(b)).

Overall, this study reveals that reducing the number of pressure measurements in the data assimilation process did not significantly impact the results. This finding was further verified by gradually decreasing the number of pressure data points considered, eventually reaching a scenario where only a single pressure measurement is considered. The detailed results of this specific case will be presented in the following subsection.

Reconstruction from a single pressure observation

Now, we examine the potential of data assimilation to accurately estimate complex turbulent mean flows using a single wall observation of the pressure coefficient (C_p) located at the chordwise coordinate $x_c = 0.4$, i.e $\bar{\mathbf{m}} = C_p(x_c = 0.4)$. We note that this position was randomly chosen. The main objective is to explore the efficacy of data assimilation in reconstructing the turbulent mean flows based on such single information. The results are illustrated in figure 4. Notably, figure 4(a) demonstrates that assimilating only a single pressure data point yields a significant recirculation region, which closely match the results obtained from DNS (see figure 1(b)). To better understand the impact of the single wall data assimilation, we analyze the gradient of the cost function $\mathcal{J}$ with respect to the model correction $\tilde{g}$ at the onset of the data assimilation process. This normalized gradient is shown in figure 4(b), revealing its distribution across the entire suction side. This distribution supports the successful reconstruction achieved with only one data point, indicating that the data assimilation procedure directly corrects the Spalart-Allmaras equation (1) over a substantial portion of the suction side, including the recirculation region. The final corrected field at the end of the data assimilation procedure is depicted in figure 4(c), presenting the quantity $\tilde{g}\tilde{\nu}/\nu$ normalized by the kinematic viscosity ν. The optimization scheme modifies the model correction $\tilde{g}$ in the opposite direction of the gradient of $\mathcal{J}$, resulting in a predominantly negative corrective forcing $\tilde{g}\tilde{\nu}$ consistent with figure 4(b). Additionally, figure 4(d) show the variation in the eddy viscosity ν_t between the assimilated and baseline RANS cases. Remarkably, the data assimilation process significantly reduces ν_t over the suction side, promoting separation. Conversely, the recovery of the recirculation region is associated with an increase in ν_t downstream of the trailing edge.

Considering the remarkable ability of data assimilation to accurately reconstruct the reference mean flow using only a single C_p data, we proceed with further analysis, focusing exclusively on this case. To investigate the effectiveness of data assimilation at a different location, we change the position of the single pressure observation to $x_c = 0.1$ on the pressure side. The data assimilation results for this new configuration are presented in figure 5. In figure 5(b), the model correction exhibits similarities to that shown in figure 4(c), leading to a similar improvement in the es-

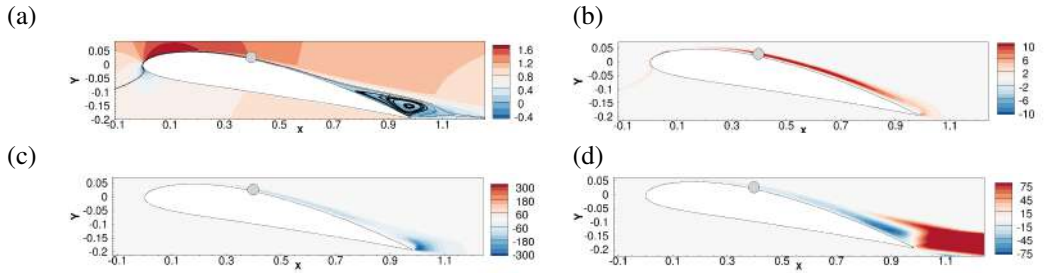

Figure 4: Data assimilation results when observing a single C_p at $x_c = 0.4$ on the suction side denoted by a grey circle. (a) reconstructed streamwise mean-velocity field, (b) normalized initial gradient $\nabla_{\tilde{g}}\mathcal{J}_0/\|\nabla_{\tilde{g}}\mathcal{J}_0\|$, (c) corrective field $\tilde{g}\tilde{\nu}/\nu$ at the end of the data assimilation procedure and (d) variation in the eddy-viscosity field $(\nu_t^a - \nu_t^b)/\nu$ between assimilated and baseline RANS.

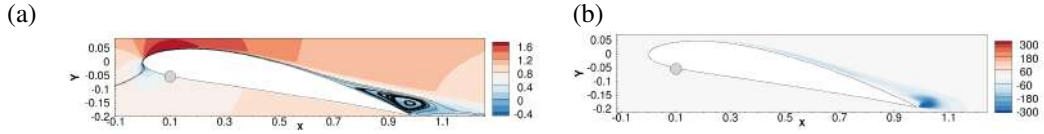

Figure 5: Data assimilation results when observing a single C_p at $x_c = 0.1$ on the pressure side denoted by a grey circle. (a) reconstructed streamwise mean-velocity field and (b) corrective field $\tilde{g}\tilde{\nu}/\nu$ at the end of the data assimilation procedure.

Relative Erros	$e_r(\tilde{\mathbf{u}})$
DA-Full state	0.081
DA-Full C_p	0.191
DA-40 C_p	0.243
DA-1 $C_p(x_c = 0.4)_s$	0.263
DA-1 $C_p(x_c = 0.1)_p$	0.260

Table 1: Relative reconstruction error of velocity $e_r(\tilde{\mathbf{u}})$ at the end of the data assimilation procedure for different cases denoted by DA. The notations of $(\,)_s$ and $(\,)_p$ used in the case of a single pressure data, correspond to the suction and pressure side respectively.

Aerodynamic coefficients	C_D	C_L
DNS	0.034	1.259
Baseline RANS	0.028	1.457
DA-Full state	0.038	1.256
DA-Full C_p	0.034	1.259
DA-40 C_p	0.033	1.262
DA-1 $C_p(x_c = 0.4)_s$	0.033	1.255
DA-1 $C_p(x_c = 0.1)_p$	0.033	1.252

Table 2: Comparison of the aerodynamics coefficient (lift and drag coefficients C_D and C_L respectively) obtained with DNS, baseline RANS and different cases of assimilation denoted by DA.

timation of the recirculation region, as can be seen in figure 5(a). This consistent improvement confirms the impressive ability of data assimilation in reconstructing the entire flow based on a single pressure data located at the pressure side. To evaluate the performance of the data assimilation results quantitatively, we calculate the relative mean velocity reconstruction error $e_r(\tilde{\mathbf{u}})$ (see equation 3) A comparison of the relative error for the different data assimilation cases is presented in table 1. It can be clearly seen that the assimilation of the full state DNS case yields the best results for velocity reconstruction, which is expected. Equally remarkable is the excellent performance of the other data assimilation cases, especially when considering a single pressure data. Notably, no big difference in the relative error values between assimilating all the available C_p points, using a limited number of them or only a single point located either on the suction or the pressure side.

Moreover, the reconstructed flow obtained through assimilating a single pressure data point exhibits also satisfactory characteristics in terms of wall shear stress and other parameters. Notably, in all the explored assimilation cases denoted as (DA) in table 2, the aerodynamic coefficients, such as the lift and drag coefficients (C_D and C_L, respectively), are accurately reconstructed and exhibit strong agreement with the DNS results. Particularly noteworthy is the substantial improvement in the lift coefficient (C_L). Upon comparing the different assimilation cases, there is no significant disparity in the coefficient values among the various tests. However, assimilating the full pressure distribution appears to provide the most effective reconstruction of these coefficients.

4 Conclusions

In this study, a variational data assimilation (DA) technique has been employed to reconstruct the turbu-

lent flow around a NACA4412 airfoil near stall conditions at a chord-based Reynolds number of $Re = 3.5 \cdot 10^5$. The main focus is to investigate the potential of DA in reconstructing the mean flow using sparse pressure observations extracted from high-fidelity DNS simulations, specifically for this non-trivial aeronautical configuration. The synthetic wall data used in this study was the pressure distribution C_p obtained from DNS. Various assimilation cases have been considered, including the observation of the full DNS mean flow, the observation of the full or limited wall pressure data, and a single pressure data initially located at $x_c = 0.4$ on the suction side. The comparison and validation have been performed using the assimilation of the full DNS mean flow.

In all the examined assimilated cases, satisfactory results have been obtained. The reconstructed velocity field, aerodynamic coefficients, and pressure coefficients have been accurately captured. The evaluation of the relative error of the velocity fields and pressure distribution confirmed the effectiveness of the data assimilation approach to reconstruct the mean flow. Notably, there were no significant differences in the error values among the different assimilation cases, which motivated us to progressively reduce the number of pressure data until reaching the minimum required data. Remarkably, changing the location of the single pressure data point to $x_c = 0.1$ on the pressure side produced similarly successful results. This suggests to verify the robustness of the data assimilation technique in accurately reconstructing the flow regardless of the specific location of the pressure data. The encouraging findings of this study highlight the potential of data assimilation in reconstructing complex aerodynamic flows.

Future work will explore the influence of noise in the input pressure data and investigate the impact of different locations of the single pressure data to the quality of reconstruction. Additionally, it will be valuable to test alternative correction approaches to the one considered in this paper ($\tilde{g}$). Moreover, assimilating other wall data, such as skin friction coefficient (C_f) measurements, should be explored. Finally, this study suggests that the need for extensive reference data for machine-learning techniques, as used in data-driven predictive turbulence models, may be alleviated if extremely sparse wall pressure information is sufficient to calibrate RANS models.

5 *

References

[1] Z. Belligoli, R. Dwight, and G. Eitelberg. Assessment of a Data Assimilation Technique for Wind Tunnel Wall Interference Corrections. *AIAA Aviation 2019 Forum*, page 0939, 2019.

[2] M. Y. Ben Ali, G. Tissot, S. Aguinaga, D. Heitz, and E. Mémin. Mean wind flow reconstruction of a high-rise building based on variational data assimilation using sparse pressure measurements. *Journal of Wind Engineering and Industrial Aerodynamics*, 231:105204, 2022.

[3] Alexander N. Brooks and Thomas J.R. Hughes. Streamline upwind/petrov-galerkin formulations for convection dominated flows with particular emphasis on the incompressible navier-stokes equations. *Computer Methods in Applied Mechanics and Engineering*, 32(1):199–259, 1982.

[4] D. P. G. Foures, N. Dovetta, D. Sipp, and P. J. Schmid. A data-assimilation method for Reynolds-averaged Navier-Stokes-driven mean flow reconstruction. *Journal of Fluid Mechanics*, 759:404–431, 2014.

[5] L. Franceschini, D. Sipp, and O. Marquet. Mean-flow data assimilation based on minimal correction of turbulence models: Application to turbulent high reynolds number backward-facing step. *Physical Review Fluids*, 5:094603, Sep 2020.

[6] V. Gleize, M. Costes, and I. Mary. Numerical simulation of NACA4412 airfoil in pre-stall conditions. *International Journal of Numerical Methods for Heat & Fluid Flow*, 32:1375–1397, 2022.

[7] F. Hecht. New development in FreeFem++. *Journal of Numerical Mathematics*, 20:251–265, 2012.

[8] H. Kato, A. Yoshizawa, G. Ueno, and S. Obayashi. A data assimilation methodology for reconstructing turbulent flows around aircraft. *Journal of Computational Physics*, 283:559–581, 2015.

[9] S. Li, C. He, and Y. Liu. A data assimilation model for wall pressure-driven mean flow reconstruction. *Physics of Fluids*, 34:015101, January 2022.

[10] Maxim Olshanskii, Gert Lube, Timo Heister, and Johannes Löwe. Grad–div stabilization and subgrid pressure models for the incompressible navier–stokes equations. *Computer Methods in Applied Mechanics and Engineering*, 198(49-52):3975–3988, 2009.

[11] A. Singh and K. Duraisamy. Using field inversion to quantify functional errors in turbulence closures. *Physics of Fluids*, 28:045110, 04 2016.

[12] P. R. Spalart and S. R. Allmaras. A one-equation turbulence model for aerodynamic flows. *La Recherche Aérospatiale*, 1:5–21, 1994.

[13] H. Xiao and P. Cinnella. Quantification of model uncertainty in RANS simulations: A review. *Progress in Aerospace Sciences*, 51:1–31, 2019.